

## Analysis of Degradation Rate for Dimensionless Surface Area of Well-Interconnected PCL Scaffold Via in-vitro Accelerated Degradation Experiment

Se-Hwan Lee<sup>1</sup>, Jun Hee Lee<sup>2</sup>, and Young-Sam Cho<sup>1\*</sup>

<sup>1</sup>*Division of Mechanical and Automotive Engineering, College of Engineering, Wonkwang University, 460 Iksandae-ro, Iksan, Jeonbuk 570-749, Korea*

<sup>2</sup>*Nature-Inspired Mechanical System Team, Nano Convergence & Manufacturing Systems Research Division, Korea Institute of Machinery and Materials (KIMM), 104 Sinseongno, Yuseong-gu, Daejeon 305-343, Korea*

(Received: July 23<sup>th</sup>, 2014; Revision: September 2<sup>nd</sup>, 2014; Accepted: September 6<sup>th</sup>, 2014)

**Abstract :** Until now, many researchers have explained the degradation rate of biodegradable scaffold with respect to several parameters such as porosity, pore size, and strand diameter. In this study, to analyze the degradation rate of Polycaprolactone (PCL) scaffold, accelerated degradation experiment using sodium hydroxide (NaOH) was used. For the experiment, PCL scaffolds were fabricated by bioplotter with respect to porosity, pore size, and strand diameter, respectively. Each fabricated scaffold was put into a vial filled with 5 mol-NaOH 5 mL and trapped-air was removed using vacuum desiccator. After that, all vials were placed in the waterbath which was maintained with 37°C For 24 days, seven vials were taken out from the waterbath for every 2 days and each scaffold was dried after rinsing with D.I. water. Afterwards, the degradation rate was analyzed for each type of PCL scaffolds using the measured mass. Among them, one type of scaffolds, which has the strand diameter of 300  $\mu\text{m}$  and the pitch between strands of 800  $\mu\text{m}$ , was used for the measurement of molecular weight change via gel permeation chromatography (GPC). To show the each conventional parameter could not explain alone the degradation rate, the calculated degradation rates were analyzed with respect to porosity, pore size, and strand diameter, respectively. Afterwards, every degradation rate of all types of scaffolds was recorded with respect to the dimensionless surface area which is surface area/ $S_0$ .  $S_0$  is the surface area of sphere which has same volume of respective scaffold. Consequently, the dimensionless surface area was found to be a single parameter irrelevant to the type of PCL scaffold to explain the in-vitro degradation rate of accelerated NaOH experiment.

**Key words:** PCL scaffold; accelerated degradation; degradation rate; governing parameter; bio-plotter scaffold

### 1. Introduction

As mentioned in previous studies of tissue engineering, scaffold is one of key items in tissue engineering and can provide a certain 3D topological guide during tissue regeneration.<sup>1</sup> Method for 3D scaffold manufacturing has been developed and could divide conventional method and solid freeform fabrication (SFF) technique. The representative conventional methods, such as solvent casting/particulate leaching<sup>2</sup>, phase separation<sup>3</sup>, gas-foaming<sup>4</sup>, and freeze-drying<sup>5</sup>, can simply fabricate 3D porous scaffold. However, the conventional methods are difficult to control pore geometry and

interconnectivity. In contrast, SFF technique, such as 3D printing<sup>6-8</sup>, selective laser sintering<sup>9</sup>, stereo lithography<sup>10</sup>, can fabricate 3D scaffold with well-defined pore geometry and certain interconnectivity.

Until now, several synthetic polymers, which are Polyglycolic acid (PGA), Polylactic acid (PLA), Poly(lactic-co-glycolic acid) (PLGA), and Polycaprolactone (PCL), have been widely used for the scaffold fabrication.<sup>11-13</sup> Generally, implanted scaffold which is fabricated using synthetic polymers is degraded during from several months to several years with respect to material types or fabricated structures. Especially, according to Lam's study in 2008<sup>14</sup>, PCL scaffold which is fabricated by FDM (Fused Deposition Modeling) needs several years to degrade completely in simulated physiological conditions.

\*Corresponding author

Tel: +82-63-850-6694; Fax: +82-63-850-6691

e-mail: youngsamcho@wku.ac.kr (Young-Sam Cho)

Degradation rate (speed) of scaffold is important because of several reasons as follows. The newly generated space and surface by degradation are essential for the proliferation and differentiation of cells. Newly generated interconnected space by degradation could act like a channel for the exchange of nutrients and wastes. The stiffness of scaffold could be generally weakened as the scaffold is degraded. For this reason, many researches about degradation of scaffold have been conducted using in-vitro physiological simulated phosphate buffered saline (PBS) solution.<sup>15-19</sup> However, synthetic polymers having slow degradation characteristic, which are represented by PCL, are too hard to assess in a limited period. Therefore, several researches about accelerated degradation have been proposed using fluid flow<sup>20</sup>, using amine<sup>21</sup>, using poly (aspartic acid-co-lactide) (PAL)<sup>22</sup>, and using NaOH.<sup>14</sup> Among them, Lam *et al.*<sup>14</sup> compared the accelerated experiment using NaOH with the non-accelerated experiment under the physiological simulated condition. Also, according to several researches<sup>23-27</sup>, accelerated experiments using NaOH is more suitable than those using enzyme in the case of large molecular weight ( $M_n > 5000$ ).<sup>28</sup>

C. M. Agrawal *et al.*<sup>20</sup> assessed the degradation experiments using salt-leaching poly(lactide-co-glycolide) (PLG) scaffold and 37°C PBS solution and showed the result that lower porosity and permeability contribute the faster degradation rate. L. Wu *et al.*<sup>15</sup> used PLGA particulate leaching scaffold and 37°C PBS solution for the degradation experiments. In the result of Wu's study, the higher porosity gives the lower degradation rate. Moreover, the lower pore size gives the lower degradation rate.

As mentioned above, several researches have been conducted for the degradation characteristics with respect to several parameters such as porosity, pore size, and etc. However, there is no research to explain the degradation with respect to a single parameter. Because the porosity, the pore size, and the strand diameter are coupled to each other, it is obvious that they could not be a single parameter to explain the degradation characteristics. Therefore, in this study, using well-interconnected and well-defined PCL scaffolds fabricated by SFF technique, accelerated degradation experiments were conducted to reveal the single parameter to explain the degradation rate. Used SFF equipment was bioplotter which was developed by Korea Institute of Machinery and Materials (KIMM). Bioplotter can change the size of extrude nozzle and three different nozzles having 300, 350, and 400- $\mu\text{m}$  inner diameter were used and heating temperature was controlled as 100°C and working pressure was 450 MPa.

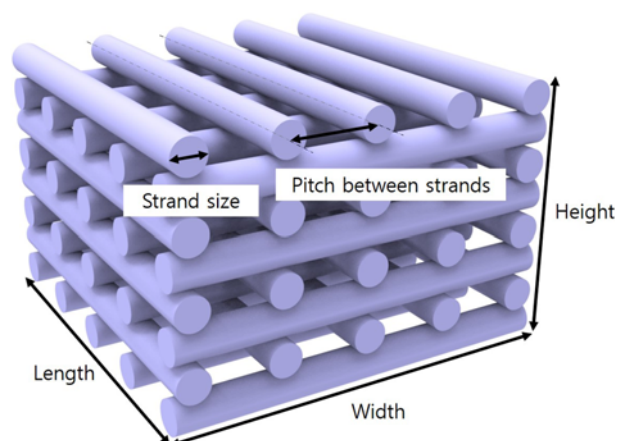


Figure 1. Illustration to explain geometrical parameters for the 3D scaffold fabrication.

Table 1. Porosities of fabricated scaffolds with respect to the strand size and pitch between strands

Strand size ( $\mu\text{m}$ )	Pitch between strands ( $\mu\text{m}$ )	Porosity (%)
300	1200	80.4
300	800	70.5
300	600	60.7
300	475	50.4
400	630	50.1
350	550	50.0

## 2. Materials & Methods

### 2.1 Materials

In this study, PCL (Polycaprolactone,  $M_n = 70,000\text{--}80,000$ , Sigma-Aldrich) was used for the scaffold fabrication. For the in-vitro environment, digital waterbath (JSWB-22T, JSR) having an accuracy of  $\pm 0.2 \times \text{C}$  at 37°C. For the accelerated experiment, 5 mol/L NaOH solution (Sodium hydroxide solution, Samchun chemicals) was used. To measure the weight of scaffolds, digital scale (HS204, Hansung) having 0.1 mg resolution was used. For the measurement of molecular weight change, Gel Permeation Chromatography (PL-GPC110, Polymer Laboratories) was used.

### 2.2 Fabrication of Scaffolds using Bioplotter

Using bioplotter which is one of dispensing type SFF equipment, PCL scaffolds with well-defined topology and well-interconnected pores were fabricated with geometric parameters as depicted in Table 1. Bioplotter is our lab-made SFF. The bioplotter can fabricate the 3D scaffold by dispensing

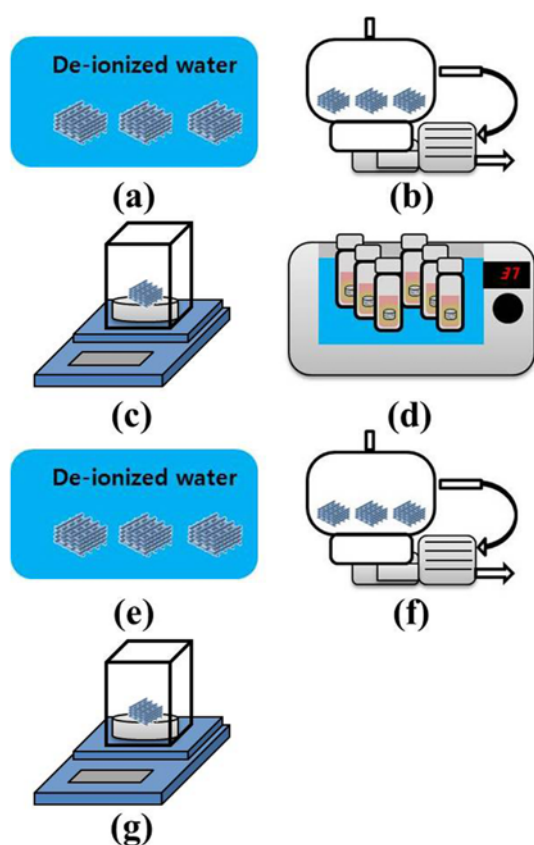


**Figure 2.** Schematics of accelerated degradation experiments using NaOH solution; (a) washing the scaffold by de-ionized water, (b) drying the scaffold in vacuum desiccator, (c) measurement of scaffold weight, (d) in-vitro accelerated degradation using waterbath and 5mol NaOH, (e) washing the degraded scaffold by de-ionized water, (f) drying the scaffold in vacuum desiccator, and (g) measurement of weight of degraded scaffold.

polymers layer-by-layer. It can control the shape, size, pore size and porosity of the 3D scaffold. To explain parameters for scaffold fabrication, the strand diameter and pitch between strands shown in Fig. 1. In detail, first of all, with 300  $\mu\text{m}$ -diameter PCL strands, the pitches between strands were varied as 475, 600, and 800  $\mu\text{m}$  to make the porosities as 50, 60, and

70%. Moreover, strand diameters/pitches were varied as 350/550 and 400/630  $\mu\text{m}$ , respectively to have the same porosity as 50%. All scaffolds have dimensions with  $5 \times 5 \times 5 \text{ mm}^3$ .

### 2.3 in-vitro Accelerated Degradation Experiment using NaOH Solution

For the accelerated degradation experiment, every 7 scaffolds were prepared with respect to scaffold types depicted in Table. 1. Prepared scaffolds were cleansed with D.I. water and dried as shown in Fig. 2(a) and (b). The weights of scaffolds were measured by digital scale for the evaluating initial weight of scaffolds as Fig. 2(c). After that, every scaffold was put into glass vials having 5 mol-NaOH solution and vials were laid in the 37°C-controlled waterbath as depicted in Fig. 2(d). Every 7 scaffolds were took out from the waterbath per every 2 days and cleansed with D.I. water and dried as depicted in Fig. 2(e) and (f). The weights of every dried 7 scaffolds were measured by digital scale as depicted in Fig. 2(g). Moreover, one scaffold type of which strand diameter/pitch is 300/800  $\mu\text{m}$  was used for the measurement of molecular weight change using GPC. Moreover, this type of scaffolds was used to analyze the topological change by optical microscope as shown in Fig. 3.

## 3. Results and Discussions

### 3.1 Analysis of Topological Change during Degradation

After accelerated degradation experiments, one type of scaffolds, which has the strand diameter/pitch as 300/800  $\mu\text{m}$ , was selected as a representative sample for the topological analysis and the molecular weight change measurement. As shown in Fig. 3, because the used scaffolds have well-interconnected pores and well-defined structures, degradation has been occurred uniformly regardless of position. Inner and outer strands have almost same diameters after degradation. However, at the each junction which is a cross point of strands, the degradation rate seems to be slower than other point of

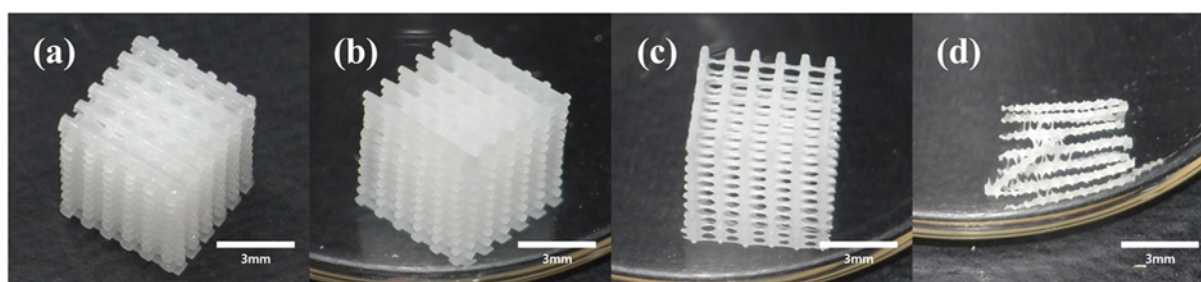


**Figure 3.** Optical images for degraded scaffolds having strand diameter/pitch of 300/800  $\mu\text{m}$ : (a) not degraded, (b) 11-day degraded, (c) 16-day degraded, and (d) 22-day degraded.

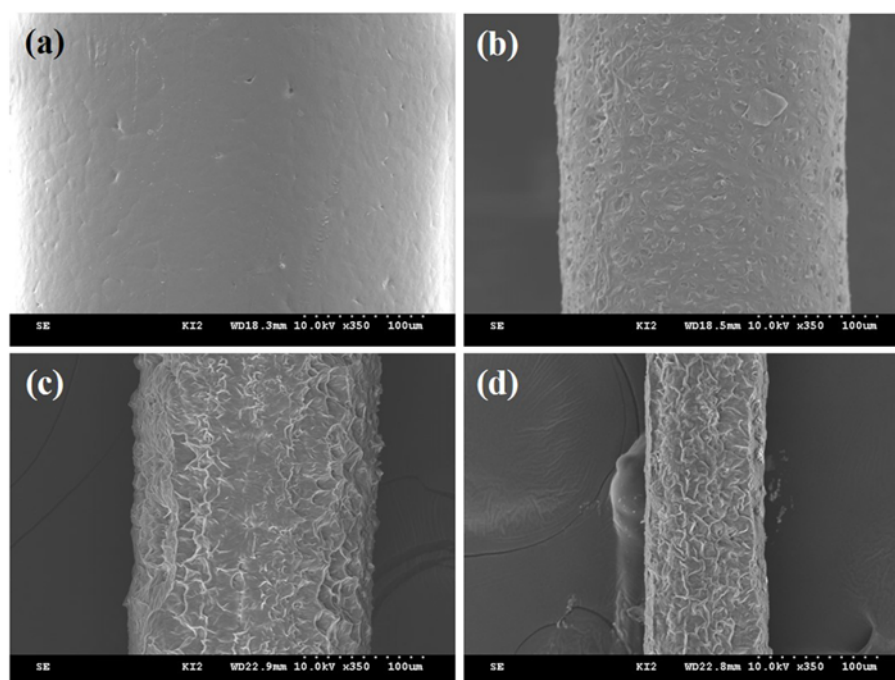


Figure 4. FE-SEM images for degraded scaffold: (a) not degraded, (b) 7-day degraded, (c) 14-day degraded, and (d) 18-day degraded.

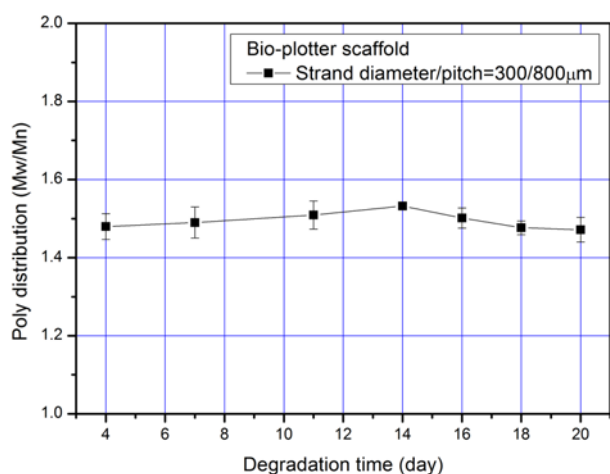


Figure 5. Poly distributions of PCL scaffolds by GPC (n = 5).

strands. This phenomenon could be explained as the result of which the surface area to volume at the junction is relatively small compared with regular point of strands. This hypothesis is going to be a clue to find the single parameter to explain the degradation rate of scaffolds in Ch. 3.5.

The degraded scaffold having strand diameter/pitch of 400/630  $\mu\text{m}$  was observed using FE-SEM (S-4800 + EDS, Hitachi) to check the morphological change in detail. As shown in Fig. 4, wrinkles were formed on the surface of degraded scaffold. It could be explained as the fragmentation of crystalline regions

during surface erosion degradation.<sup>20</sup>

### 3.2 GPC Results

As mentioned in Ch. 3.1, one type of scaffolds, which has the strand diameter/pitch as 300/800  $\mu\text{m}$ , was selected as a representative sample for the molecular weight change measurement. Each 5 scaffolds per 2 days after cleansing and drying were used for GPC experiments. For the GPC solvent, HPLC-level chloroform was used. As a result, poly distribution (Mw/Mn) was analyzed as shown in Fig. 5. As depicted in Fig. 5, the value of poly distribution was not changed with respect to the degradation time. This result could be understood as a typical output of NaOH accelerated experiment.<sup>14</sup> In the accelerated experiment using NaOH, it is assumed that the broken chain of polymer at the surface was dissolved into the medium relevant rapidly before swelling.

### 3.3 Calculation of Degradation Rates

For the calculation of degradation rate, initial weight and the remained weight after degradation were used with respect to scaffold types. First of all, for each type of scaffold, every five scaffolds were took out, cleansed, and dried per every 2 days. The weights of every seven scaffolds were measured using digital scale with 0.1 mg resolution. After that, the relative remained weights which defined as Eq. (1) were calculated using the initial weight of each scaffold. After 24 days experiment, the relative remained weights are plotted with respect to the degradation times as Fig. 6. Using simple linear

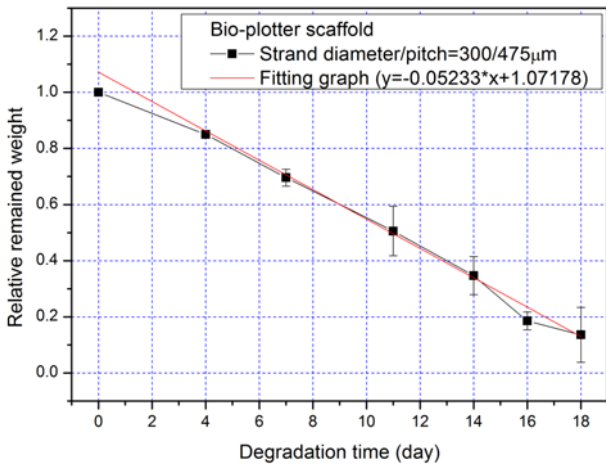


Figure 6. Relative remained weight of PCL scaffold with strand diameter/pitch = 300/475 μm (n = 7).

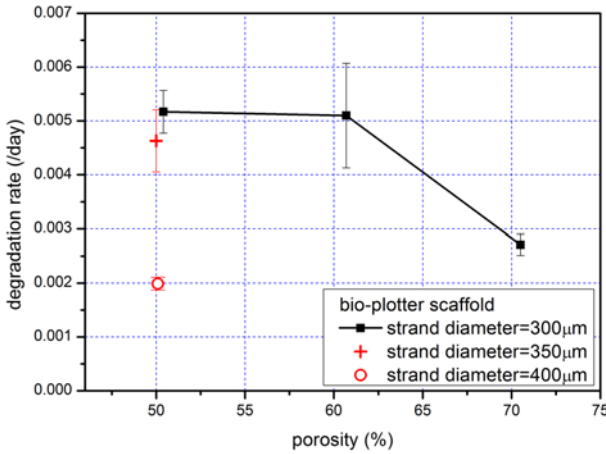


Figure 7. Comparison of degradation rate with respect to porosity.

fitting algorithm, the degradation rate which is defined as “the relative remained weight/time” was calculated as depicted in Fig. 6. For example, as shown Fig. 6, the absolute value of gradient value, 0.05233 is the degradation rate of the case of 300/475 μm (strand diameter/pitch).

$$\frac{M_d}{M_i} = M_{rel} \quad (1)$$

Where,  $M_d$  is the weight of degraded scaffold,  $M_i$  is the initial weight of scaffold, and  $M_{rel}$  is the relative remained weight.

### 3.4 Degradation Rates with Respect to Porosity, Pore Size, and Strand Diameter

In this section, above mentioned degradation rates were analyzed with respect to porosity, pore size, and strand diameter. First of all, as shown in Fig. 7, degradation rates were plotted with respect to the porosity. The line-plotted data are

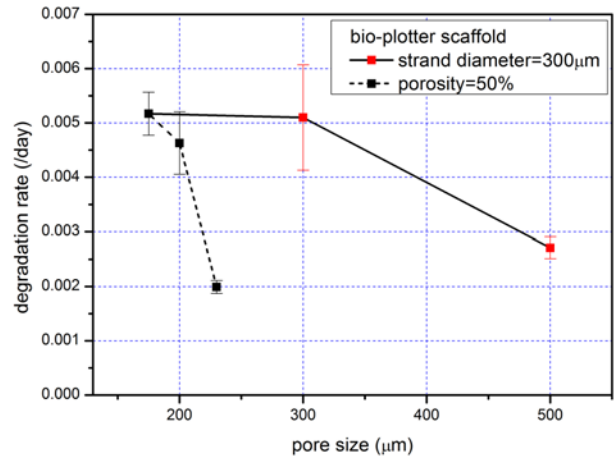


Figure 8. Comparison of degradation rate with respect to pore size.

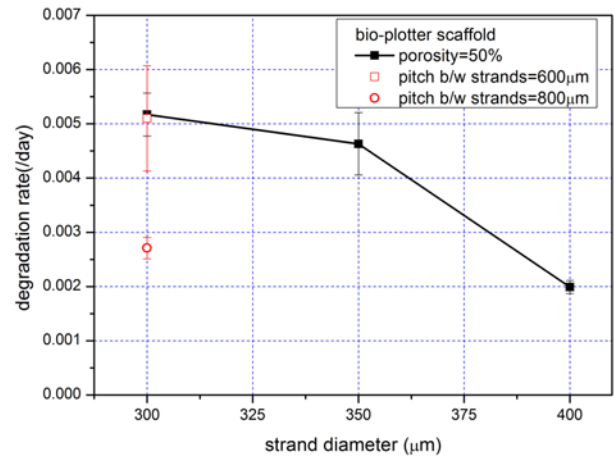
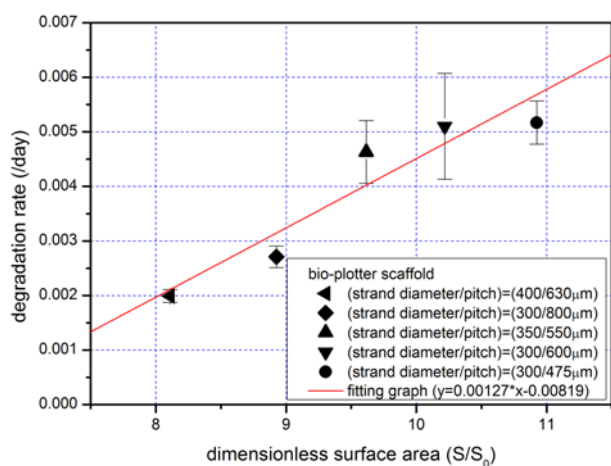


Figure 9. Comparison of degradation rate with respect to strand diameter.

related with the scaffolds having same strand diameters and different porosities because of different pitches between strands. In that case, the degradation rate became smaller as the porosity became larger. However, in Fig. 7, cross-patterned and open-circle-patterned data have different degradation rates compared with the line-patterned datum having the same porosity. Cross-patterned and open-circle-patterned data represent 350/550 μm (strand diameter/pitch) and 400/630 μm (strand diameter/pitch), respectively. Therefore, considering only Fig. 7, the degradation rates are not governed by only the porosity.

Moreover, as shown in Fig. 8, degradation rates were plotted with respect to the pore size. In this study, actually, scaffolds were designed as varying the pitch between strands. Therefore, the pore size could be assumed as the value which the pitch minus the strand diameter. The solid-line-plotted data are related with the scaffolds having same strand diameters and



**Figure 10.** Comparison of degradation rate with respect to the dimensionless surface area ( $S/S_0$ ).

different pore size because of different pitches between strands. The dashed-line-plotted data are related with the scaffolds having same porosities and different pore size because of different pitches between strands. As depicted in Fig. 8, the degradation rates are not governed by only the pore size.

Furthermore, as shown in Fig. 9, degradation rates were plotted with respect to the strand diameter. The solid-line-plotted data are related with the scaffolds having same porosity and different strand diameters. Also, open-square-patterned and open-circle-patterned data have different degradation rates compared with the line-patterned datum having the same strand diameter. Open-square-patterned and open-circle-patterned data represent 300/600  $\mu\text{m}$  (strand diameter/pitch) and 300/800  $\mu\text{m}$  (strand diameter/pitch), respectively. Therefore, considering only Fig. 9, the degradation rates are not governed by only the strand diameter.

### 3.5 Degradation Rates with Respect to Dimensionless Surface Area

As mentioned in Ch. 3.1, the degradation rate at the junction which is the cross point of two strands is slower than the other region. The surface area at the junction is relatively small compared with that at the other point of strands. Therefore, in this study, “the dimensionless surface area,” which is the surface area to  $S_0$ , is proposed as a single parameter to govern the degradation rate regardless of scaffold types.  $S_0$  means that the surface area of sphere which has same volume of respective scaffold. The surface area of each scaffold is calculated using simple arithmetic assuming the scaffold is stacked by cylinder-shape rods, because the used scaffolds were fabricated by bioplotter which is a dispensing type SFF apparatus using

circle-shape nozzle. Moreover,  $S_0$  is calculated easily from the initial weight of scaffolds and the density of PCL. Following this concept, all degradation rate data were plotted with respect to “the dimensionless surface area” in Fig. 10. As shown in Fig. 10, the degradation rate is linearly increased with respect to “the dimensionless surface area” regardless of the types of scaffolds.

## 4. Conclusions

In this study, using NaOH, accelerated degradation experiments of PCL scaffolds were conducted to find a single parameter to explain the degradation rate regardless of scaffold types. For the exact parametric studies, scaffolds were fabricated by SFF apparatus to have well-interconnected pores and well-defined structures. First of all, from the observation of topological change during degradation, a clue for the single parameter was found. In detail, the degradation rate at the junction which is the cross point of two strands is slower than the other region. Moreover, the surface area at the junction is relatively small compared with the other point of strands. Subsequently, the degradation rates were analyzed with respect to several conventional parameters such as porosity, pore size, and strand diameter. As a result, these conventional parameters could not explain the degradation rate alone because they are coupled to each other. Finally, “the dimensionless surface area” was proposed and every degradation rates were plotted with respect to the dimensionless surface area. Consequently, the degradation rate is linearly increased with respect to the dimensionless surface area regardless of the types of scaffolds.

Although this result was obtained from PCL well-defined scaffolds using accelerated experiment, it could be extrapolated to the other well-defined scaffolds fabricated by synthetic polymers having similar degradation mechanism because of the validity of NaOH accelerated experiment. To confirm the proposed hypothesis, additional experiments using another synthetic polymer well-defined scaffold should be conducted.

**Acknowledgement:** This research was supported by Basic Science Research Program through the National Research Foundation of Korea(NRF) funded by the Ministry of Science, ICT & Future Planning(2014R1A1A1007298)

**Disclosure Statement:** There are no animal experiments carried out for this article.

**Conflict of interest:** Se-Hwan Lee, Jun Hee Lee, and Young-

Sam Cho declare that they have no conflict of interest.

## References

1. E Sachlos and JT Czernuszka, Making tissue engineering scaffolds work. review on the application of solid freeform fabrication technology to the production of tissue engineering scaffolds, *European Cells Mater*, **5**, 29 (2003).
2. P Zhang, Z Hong, T Yu, X Chen, X Jing, In vivo mineralization and osteogenesis of nanocomposite scaffold of poly(lactide-co-glycolide) and hydroxyapatite surface-grafted with poly(L-lactide), *Biomaterials*, **30**, 58 (2009).
3. AS Rowlands, SA Lim, D Martin, JJ Cooper-White, Polyurethane/poly(lactic-co-glycolic) acid composite scaffolds fabricated by thermally induced phase separation, *Biomaterials*, **28**, 2107 (2007).
4. M-O Montjovent, L Mathieu, H Schmoekel, S Mark, P-E Bourban, P-Y Zambelli, LA Laurent-Applegate, DP Pioletti, Repair of critical size defects in the rat cranium using ceramic-reinforced PLA scaffolds obtained by supercritical gas foaming, *J Biomed Mater Res A*, **83A**, 41 (2007).
5. HW Kang, Y Tabata, Y Ikada, Fabrication of porous gelatin scaffolds for tissue engineering, *Biomaterials*, **20**, 1339 (1999).
6. H Seitz, W Rieder, S Irsen, B Leukers, C Tille, Three-dimensional printing of porous ceramic scaffolds for bone tissue engineering, *J Biomed Mater Res B: Appl Biomater*, **74B**, 782 (2005).
7. KH Lee, GH Jin, CH Jang, W-K Jung, GH Kim, Preparation and characterization of multi-layered poly(-caprolactone)/chitosan scaffolds fabricated with a combination of melt-plotting/in situ plasma treatment and a coating method for hard tissue regeneration, *J Mater Chem B*, **1**, 5831 (2013).
8. YB Kim, GH Kim, Collagen/alginate scaffolds comprising core (PCL)-shell (collagen/alginate) struts for hard tissue regeneration: fabrication, characterisation, and cellular activities, *J Mater Chem B*, **1**, 3185 (2013).
9. JM Williams, A Adewunmi, RM Schek, CL Flanagan, PH Krebsbach, SE Feinberg, SJ Hollister, S Das, Bone tissue engineering using polycaprolactone scaffolds fabricated via selective laser sintering, *Biomaterials*, **26**, 4817 (2005).
10. FPW Melchels, AMC Barradas, CA van Blitterswijk, J de Boer, J Feijen, DW Grijpma, Effects of the architecture of tissue engineering scaffolds on cell seeding and culturing, *Acta Biomaterialia*, **6**, 4208 (2010).
11. T Hayashi, Biodegradable polymers for biomedical uses, *Prog Polym Sci*, **19**, 663 (1994).
12. H Sun, L Mei, C Song, X Cui, P Wang, The in vivo degradation, absorption and excretion of PCL-based implant. *Biomaterials*, **27**, 1735 (2006).
13. J-H Shim, T-S Moon, M-J Yun, Y-C Jeon, C-M Jeong, D-W Cho, J-B Huh, *J Mater Sci: Mater Med*, **23**, 2993 (2012).
14. CXF Lam, MM Savalani, S-H Teoh, DW Hutmacher, Dynamics of in vitro polymer degradation of polycaprolactone-based scaffolds: accelerated versus simulated physiological conditions, *Biomed mater*, **3**, 1 (2008).
15. L Wu, J Ding, Effects of porosity and pore size on in vitro degradation of three-dimensional porous poly(D,L-lactide-co-glycolide) scaffolds for tissue engineering, *J Biomed Mater Res A*, **75A**, 767 (2005).
16. SI Jeong, B-S Kim, YM Lee, KJ Ihn, SH Kim, YH Kim, Morphology of Elastic Poly(L-lactide-co--caprolactone) Copolymers and in Vitro and in Vivo Degradation Behavior of Their Scaffolds, *Biomacromolecules*, **5**, 1303 (2004).
17. H-J Sung, C Meredith, C Johnson, ZS. Galis, The effect of scaffold degradation rate on three-dimensional cell growth and angiogenesis, *Biomaterials*, **25**, 5735 (2004).
18. JJ Yoon, TG Park, Degradation behaviors of biodegradable macroporous scaffolds prepared by gas foaming of effervescent salts, *J Biomed Mater Res*, **55**, 401 (2000).
19. A Yeo, B Rai, E Sju, JJ Cheong, SH Teoh, The degradation profile of novel, bioresorbable PCL-TCP scaffolds: An in vitro and in vivo study. *J Biomed Mater Res A*, **84A**, 208 (2007).
20. CM Agrawal, JS McKinney, D Lanctot, KA Athanasiou, Effects of fluid flow on the in vitro degradation kinetics of biodegradable scaffolds for tissue engineering, *Biomaterials*, **21**, 2443 (2000).
21. W-J Lin, DR Flanagan, RJ Linhardt, Accelerated Degradation of Poly(epsilon-caprolactone) by Organic Amines, *pharmaceutical research*, **11**, 1030 (1994).
22. U Little, F Buchanan, E Harkin-Jones, M McCaigue, D Farrar, G Dickson, Accelerated degradation behaviour of poly(3-caprolactone) via melt blending with poly(aspartic acid-co-lactide) (PAL), *Polym Degrad Stabil*, **94**, 213 (2009).
23. CG Pitt, FI Chasalow, YM Hibionada, DM Klimas, A Schindler, Aliphatic polyesters. 1. The degradation of poly(epsilon-caprolactone) in vivo, *J Appl Polym Sci*, **26**, 3779 (1981).
24. M Therin, P Christel, S Li, H Garreau, M Vert, In vivo degradation of massive poly(alpha-hydroxyacids) validation of in vitro findings, *Biomaterials*, **13**, 594 (1992).
25. AS Htay, SH Teoh, DW Hutmacher, Development of perforated microthin poly(epsilon-caprolactone) films as matrices for membrane tissue engineering, *J Biomater Sci Polym Ed*, **15**, 683 (2004).
26. YC Kim, HS Jun, HN Chang, SI Woo, Optimal Conditions for Enzymatic Degradation of Polycaprolactone, *J Korean Chem Eng Res*, **30**, 718 (1992).
27. MA Woodruff, DW Hutmacher, The return of a forgotten polymer-Polycaprolactone in the 21st century, *Prog Polym Sci*, **35**, 1217 (2010).
28. AS Htay, SH Teoh, DW Hutmacher, Development of perforated microthin poly(ε-caprolactone) films as matrices for membrane tissue engineering, *J. Biomater. Sci. Polymer Edn*, **15**, 683 (2004).